On excitons and other gap states in boron carbide

On excitons and other gap states in boron carbide

H Werheit

Institute of Physics, University Duisburg-Essen, Campus Duisburg, D-47048 Duisburg, Germany

E-mail: helmut.werheit@uni-duisburg-essen.de and helmut.werheit@koeln.de

Abstract
The excitons in boron carbide recently independently proved to be present
by luminescence measurements (by Schmechel and co-workers) and by x-ray
Raman scattering investigations in connection with *ab initio* calculations (by
Feng and co-workers) are discussed, taking the actual structure of boron carbide
within the homogeneity range ($B_{4.3}C$–$B_{\sim 11}C$) into account. The excitonic levels
at 1.560 and 1.5695 eV obtained from the luminescence spectrum are attributed
to the central B atom in the C–B–C and the C–B–B chains respectively.
Considering the transition energies related to the different gap states obtained by
optical and electrical measurements for energies below the interband transition
of 2.09 eV, an actualized energy band scheme of boron carbide is presented.

1. Introduction

Boron carbide, often incorrectly denoted as B_4C, belongs to the structure group of α-
rhombohedral boron within the icosahedral boron-rich solids. Its homogeneity range extends
from $B_{4.3}C$ at the carbon-rich limit to $B_{\sim 11}C$ at the boron-rich limit. The compound B_4C does
not exist. This was proved by Schwetz and Karduck [1] for the first time, and has been since
confirmed by numerous other experimental investigations (see [2], and references therein).
If this chemical composition is obtained, it consists of the compound $B_{4.3}C$ and precipitated
graphitic free carbon. Therefore, in particular close to the carbon-rich limit of the homogeneity
range, for a reliable chemical analysis of boron carbide the separate analysis of bonded and free
carbon in the structure is indispensable [3].

In boron carbide, there is no unit cell representing the whole structure like in common
crystalline solids. Within the whole homogeneity range, the structure is characterized by
elementary cells, which are nearly isomorphous only. They are composed of 12-atomic, by the
Jahn–Teller effect slightly distorted B_{12} or $B_{11}C$ icosahedra residing at each vertex, and mostly
three-atomic linear chains on the main cell diagonal, which is parallel to the crystallographic
c-axis. B_{12} and $B_{11}C$ icosahedra, C–B–C, C–B–B, B $\square$ B ($\square$, vacancy), and sometimes C–C–C
chains in very low concentrations only, form differently composed elementary cells that are
statistically distributed over the whole structure (see [2] and references therein, [4, 5]). This

Table 1. Concentration of structural elements in the elementary cell of boron carbide at some selected chemical compositions within the homogeneity range (see [2], [4, 5, 14, 15]).

	$B_{4.3}C$	$B_{13}C_2$	B_8C
B_{12} icosahedra	0	42	26
$B_{11}C$ icosahedra	100	58	74
C–B–C	81	62	7
C–B–B	19	19	77
B □ B (□, vacancy)	0	19	16

statistical occupation of specific atomic sites together with the very similar scattering cross sections of boron and carbon atoms for x-rays explains the failing of such investigations to determine the structural details of boron carbide.

According to theoretical calculations [6–8], the compound $B_{13}C_2$ with the hypothetical structure formula B_{12} (C–B–C), which is metallic in contrast to the real semiconducting boron carbide, is the energetically most favourable structure. Related to this theoretical structure model, the actual structures exhibit high concentrations of defects (order of magnitude, 0.1 to 1 per elementary cell corresponding to about 10^{21} cm^{-3}), which essentially determine the electronic properties by generating gap states of corresponding density. The resulting electronic structure of real boron carbide is a completely filled valence band and high density gap states partly filled by electrons coming from donors generated by C atoms substituting for B sites. The Fermi level is pinned within these split-off valence states up to very high temperatures, hence essentially determining the p-type semiconducting behaviour [9, 10]. Moreover, this extremely high concentration of defects, which is exceptional for a crystalline solid, easily explains many unusual properties of boron carbide, for example the glass-like thermal conductivity (see [2] and references therein).

Recently, the existence of excitons in boron carbide was proved in two independent studies: Photoluminescence spectra showed the existence of a stronger excitonic level at 1.56 eV and a weaker one near 1.57 eV in the 2.1 eV band gap of boron carbide [11]. X-ray Raman scattering (XRS) in combination with site-specific *ab initio* calculations identified a near-edge peak as a p-type exciton due to dominant boron occupation in the centre of the elementary cell [12]. On the basis of both papers and considering other results, in particular the actual structure of boron carbide, several further conclusions on the excitons are presented below.

Taking the transition energies derived from optical absorption and high temperature electrical conductivity additionally into account, the energy band scheme of boron carbide can be compiled allowing consistency in describing largely all available experimental results.

2. Excitons

The summarizing interpretation of experimental luminescence [11], optical absorption [20, 21], XRS [12] results, and site-specific *ab initio* calculations [12] yields a consistent and rather detailed picture of the excitons in boron carbide, which according to [12] are to be attributed to p-type core excitons from the central B atoms in the three-atomic chain in the elementary cell. The reinterpretation is based on the actual distribution of structural elements in the boron carbide structure, which was determined by the evaluation of phonon spectra (IR and Raman) and in parts confirmed by neutron scattering [13]. For some boron carbide compounds the actual concentration of structural elements is listed in table 1 (see [2]; [4, 5, 14, 15]).

The photoluminescence spectrum presented in [11] is refitted considering the attribution to a p-type core exciton at the central B atom [12] in the elementary cell, and accordingly taking
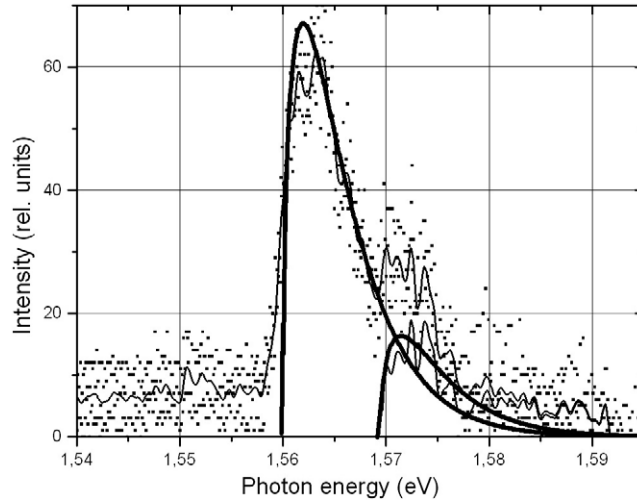
Figure 1. $B_{4.3}C$, photoluminescence spectrum at 290 K [11]. Excitation with the 514.5 nm (2.4 eV) line of an Ar laser; intensity 280 mW mm^{-2}. Squares, experimental results; thin lines, averaged experimental results, before and after subtracting the 1.56 eV model fit respectively; thick lines, recombination models of free excitons (1.560 and 1.5695 eV respectively).

into account that a certain difference for the exciton bond energy in C–B–C and in C–B–B chains should be expected. Indeed, the main luminescence maximum can be well fitted by two transition processes representing the indirect allowed recombination of free excitons [16]:

$$I(\omega) \propto \sqrt{\hbar\omega - E_0} \cdot \exp[(\hbar\omega - E_0)/k_B T_e]$$

with $E_{01} = 1.560$ eV and $E_{02} = 1.5695$ eV respectively, and the exciton temperatures $T_e = 46$ K as the only additional parameter for fitting (figure 1). The relation of the integrals of the fits E_{01}/E_{02} is 4.1 in good agreement with the relation of the chain concentrations C–B–C/C–B–B = 4.26 (see table 1). This suggests attributing the 1.560 eV excitons to the central B atom in the C–B–C and the 1.5695 eV excitons to the central B atom in the C–B–B chains.

As worked out in [11] in some detail, the experimentally determined indirect band gap of 2.09 eV for boron carbide [20] yields the exciton bond energy of about 500 meV. Using the dielectric constant $\varepsilon_r \approx 10$ (see [2]), a carrier effective mass of the order of 10 m_0 is obtained, which agrees quite well with the evaluation of the dynamical conductivity of boron carbide [17, 18], EPR [19], and several other experimental and theoretical investigations (see [2] and references therein).

The high resolution optical absorption spectrum of polycrystalline boron carbide and the XRS spectrum, compared in figure 2, agree quite well; in particular, if the relatively low resolution of the monochromatic beam used in the XRS spectrometer (1.3 eV according to [12]) is taken into account. The isotherms of the optical absorption show that the excitonic level is stable at temperatures below ~540 K only.

The excitonic level at 1.560 eV easily explains the much higher optical absorption of the high quality boron carbide single crystal in this spectral range [21] compared with the spectra of polycrystalline material [20] (see figure 2). Obviously, the probability of exciton generation is considerably reduced by extrinsic structural distortions in polycrystalline boron carbide.
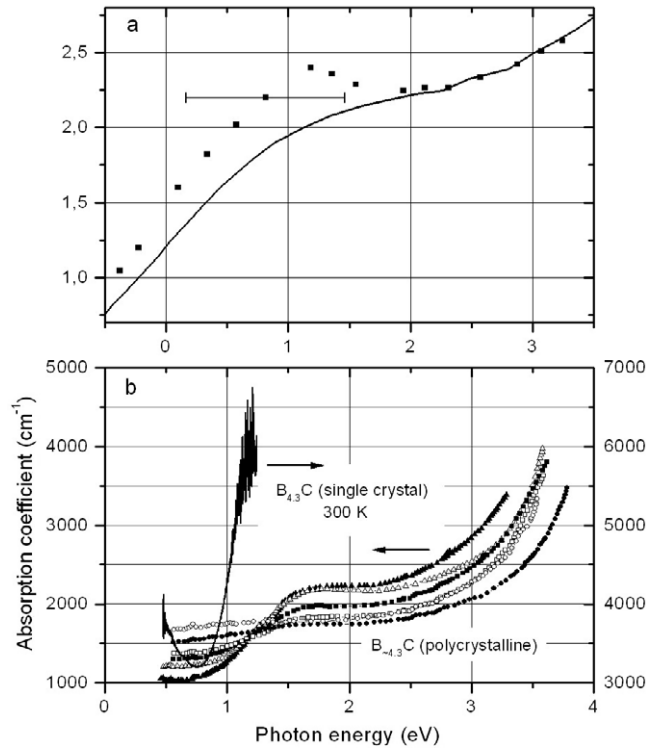
Figure 2. $B_{4.3}C$. (a) X-ray Raman scattering (XRS) spectrum [12]. Symbols, selected experimental data for $q = 1.05$ Å^{-1} (the bandwidth of the monochromatic beam is marked as horizontal error bar); line, site-specific *ab initio* calculation for the background of icosahedral B atoms. We assume that the composition of this boron carbide corresponds to $B_{4.3}C$, the carbon-rich limit of the homogeneity range; the composition B_4C claimed by the authors does not exist (see the introduction). (b) Optical absorption edge [20, 21]. Symbols, polycrystalline material (solid triangle, 80 K, sample not in thermal equilibrium; open triangle, 300 K; solid square, 300 K; open square, 360 K; solid circle, 540 K; open circle, 590 K); full line, high quality single crystal. In the 590 K spectrum a systematic error in the original publication resulting from the thermal emission of the sample is corrected.

3. Transition energies

The evaluation of the optical absorption edge yields precise transition energies of electrons in semiconductors. Reliable theoretical models [22, 23] allow fitting the experimental data, and the different energy dependences allow deciding about the type of transition.

Several low energy transitions in boron carbide were at first attributed to indirect allowed interband transitions [20]. However, the evidence of high density localized states in the band gap of boron carbide required a reinterpretation [9, 10], though the energy dependences of the optical absorption coefficient α for indirect allowed interband transitions and nondirect transitions between band-type and localized states

$$(\alpha \sim (\hbar\omega \pm k\Theta - \Delta E)^2/\hbar\omega)$$

are the same apart from the fitting parameter $k\Theta$ having no influence on the energy dependence. The accordingly newly attributed optical transitions up to the interband transition energy $\Delta E = 2.09(1)$ eV between valence and conduction band are listed in table 2. The energy of transition

Table 2. Electron transition energies of boron carbide, experimentally determined by optical absorption, photoabsorption, electrical conductivity, Hall effect.

| Opt. abs. [20] polycryst.	Opt. abs. [24] polycryst.	Opt. abs. [21] monocryst.	Opt. abs. [18] polycryst.	Photoab- sorption [24]	Electr. conduct. [26]	Hall effect (see [25])	Type of transition
			0.065(5)		0.068(5)	0.061(7)	Valence band—acceptor
0.18(1)					0.15(3)		Deep level to band
				0.27(1)			El.-trap—conduction band
0.47(1)	0.48(3)				0.46(3)		Nondirect
0.77(1)		0.76(1)					Nondirect
0.92(1)		0.93(1)					Nondirect
1.20(1)							Nondirect
2.09(1)							Indirect allowed interband

between an electron trapping level and the conduction band obtained from photoabsorption measurements at 113 K [24] is given as well. However, the donor level predicted in [9, 10] to result from antisite defects in boron carbide is not marked because it has not yet been experimentally verified.

Concerning the determination of transition energies, the electrical conductivity has hitherto not been sufficiently taken into account. While at lower temperatures the electrical conductivity follows Mott's law of variable-range hopping in a large range (see [2], and references therein), at high temperatures it is obviously thermally activated in different processes depending on temperature. In figure 3 the conductivity data reported by Wood [26, 27] are displayed, which are well compatible with measurements of other groups (see [2] and references therein). The activation energies obtained by fitting the experimental data are listed in table 2 as well. Obviously, up to about 400 K the Fermi level is positioned within the acceptor level, 0.065 eV above the valence band edge. When the thermal activation energy is sufficiently high, it is shifted to the 0.18 eV level, where it remains between 400 and 580 K. Between 1150 and 1800 K it is pinned in the 0.47 eV level. In these ranges the conductivity increases because of the thermal generation of further free holes by the thermal excitation of electrons into the particular gap states. In the intermediate ranges the electrical conductivity only weakly depends on temperature because the thermal energy is not sufficient to excite electrons remarkably into the next level. Such an intermediate range is also indicated at the high temperature end of the range of measurements between 2000 and 2400 K. This makes clear that below the melting point of about 2600 K in boron carbide no intrinsic conductivity with thermal excitation across the band gap is possible. There seem to be no essential differences for boron carbides of different compositions within the homogeneity range. This is not surprising because not the kind but only the concentration of structural defects (see table 1) depends on the actual compound.

The determination of the excitonic level allows completing the energy band scheme of boron carbide (figure 4). The deep levels split off from the valence band were determined by analysing the optical absorption edge [20]. Those at lower energies were satisfactorily confirmed by the activation energies obtained from the electrical conductivity at high temperatures [2] as shown in figure 3. The attribution of the 0.47 eV transition determined by optical absorption to a deep level associated to the valence band, and not to the separation of the excitons ($\sim$0.5 eV) is strongly supported by the electrical conductivity confirming this thermal activation energy in a high temperature range, where the excitons are no more stable according to the optical absorption spectra in figure 2.
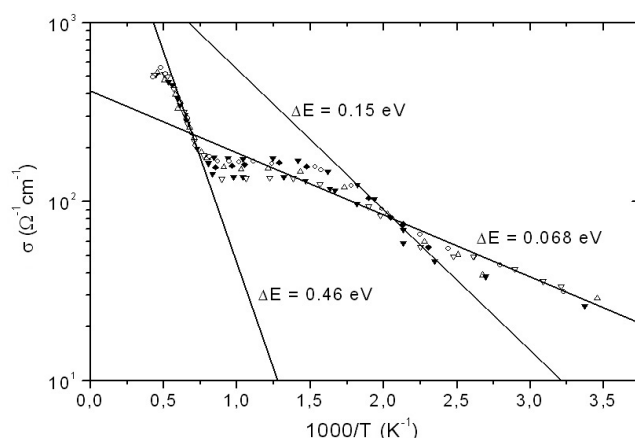
Figure 3. Boron carbide. High temperature electrical conductivity; selected results [26, 27]. The data represent $B_{13}C_2$, and the different symbols show the results on one specific, but nevertheless representative sample and were obtained in several heating and cooling cycles before and after annealing at 750 °C. For other compositions of boron carbide the electrical conductivity exhibits qualitatively similar and only quantitatively differing results. The thermal activation energies only weakly depend on the composition (see [37]). The results presented are compatible with those published by other authors (see [2] and references therein, [28, 29]).
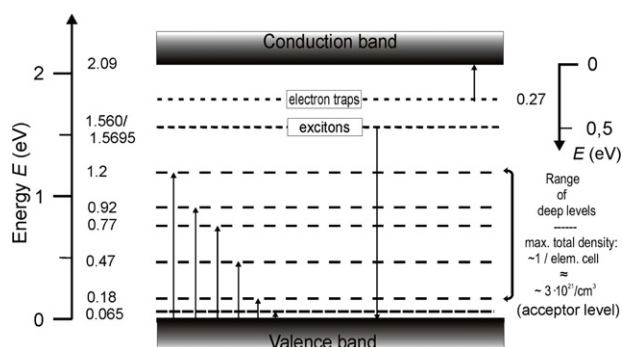
Figure 4. Boron carbide. Energy band scheme based on optical absorption, luminescence, XRS, and transport properties. Left ordinate, energies related to the valence band edge; right ordinate, energies relative to the conduction band edge. Arrows indicate the direction of the measured optical transition.

The attribution of the absorption band with maximum close to 1.5 eV to the excitons completes the absorption processes within the absorption edge of boron carbide.

This conventional band scheme for boron carbide is in contrast to the bipolaronic hopping picture proposed by Emin *et al* [30–36], which is critically discussed in a separate paper [37].

4. Conclusion

On the basis of the energy of the excitons in boron carbide and the different transition energies derived from optical absorption, photoabsorption and temperature-dependent electronic transport, the energy band scheme displayed in figure 4 is obtained. As shown, the band scheme allows consistency in describing at least most of experimental results hitherto obtained.

For electronic transitions at higher photon energies derived from optical absorption and interband critical points between 2.5 and 9.5 eV determined by measurements with a VUV ellipsometer the reader is referred to [20] and [38] respectively.

References

[1] Schwetz K A and Karduck P 1990 Investigations in the boron–carbon system with the aid of electron probe microanalysis *AIP Conf. Proc.* **231** 405–13

[2] Werheit H 2000 Boron compounds *Numerical Data and Functional Relationships in Science and Technology* (*Landolt–Börnstein New Series* Group III, vol 41D) ed O Madelung (Berlin: Springer) pp 1–491

[3] Schwetz K A and Hassler J 1986 A wet chemical method for the determination of free carbon in boron carbide, silicon carbide, and mixtures thereof *J. Less-Common Met.* **117** 7

[4] Werheit H, Au T, Schmechel R, Shalamberidze S O, Kalandadze G I and Eristavi A M 2000 IR active phonons and structure elements of isotope-enriched boron carbide *J. Solid State Chem.* **154** 79

[5] Werheit H, Rotter H W, Meyer F D, Hillebrecht H, Shalamberidze S O, Abzianidze T G and Esadze E G 2004 FT–Raman spectra of isotope-enriched boron carbide *J. Solid State Chem.* **177** 569–74

[6] Bylander D M and Kleinman L 1990 Self-consistent calculations of the energy bands and bonding properties of $B_{13}C_2$ *Phys. Rev.* B **42** 1394

[7] Bylander D M and Kleinman L 1991 Structure of $B_{13}C_2$ *Phys. Rev.* B **43** 1487

[8] Kleinman L 1991 *Ab initio* calculations of boron and its carbides *AIP Conf. Proc.* **231** 13

[9] Schmechel R and Werheit H 1999 Correlation between structural defects and electronic properties of icosahedral boron-rich solids *J. Phys.: Condens. Matter* **11** 6803–13

[10] Schmechel R and Werheit H 2000 Structural defects of some icosahedral boron-rich solids and their correlation with the electronic properties *J. Solid State Chem.* **154** 61–7

[11] Schmechel R, Werheit H, Kampen T U and Mönch W 2004 Photoluminescence in boron carbide *J. Solid State Chem.* **177** 566–8

[12] Feng Y, Seidler G T, Cross J O, Macrander A T and Rehr J J 2004 Role of inversion symmetry and multipole effects in nonresonant x-ray Raman scattering from icosahedral B_4C *Phys. Rev.* B **69** 125402

[13] Kwei G H and Morosin B 1996 Structures of the boron-rich boron carbides from neutron powder diffraction: Implications for the nature of inter-icosahedral chains *J. Phys. Chem.* **100** 8031

[14] Kuhlmann U and Werheit H 1992 On the microstructure of boron carbide *Solid State Commun.* **83** 849

[15] Kuhlmann U, Werheit H and Schwetz K A 1992 Distribution of carbon atoms on the boron carbide structure elements *J. Alloys Compounds* **189** 249

[16] Bebb H H and Williams E W 1972 Photoluminenence I: theory *Semiconductors and Semimetals* vol 8 *Transport and Optical Phenomena* ed R K Williardson and A C Beer (London: Academic) p 182

[17] Schmechel R and Werheit H 1997 Evidence of the superposition of Drude type and hopping type transport in boron-rich solids *J. Solid State Chem.* **133** 335

[18] Schmechel R and Werheit H 1998 Dynamical transport in icosahedral boron-rich solids *J. Mater. Process. Manufact. Sci.* **6** 329

[19] Geist D, Meyer J and Peussner H 1970 Electrical conductivity and movable carrier electron paramagnetic resonance (EPR) *Boron* vol 3, ed T Niemyski (Warsaw: PWN) pp 207–14

[20] Werheit H, Laux M, Kuhlmann U and Telle R 1992 Optical interband transitions of boron carbide *Phys. Status Solidi* b **172** K81–6

[21] Werheit H, Leithe-Jasper A, Tanaka T, Rotter H W and Schwetz K A 2004 Some properties of single-crystal boron carbide *J. Solid State Chem.* **177** 575–9

[22] Smith R A 1961 *Wave Mechanics in Crystalline Solids* (London: Chapman and Hall)

[23] Lucovsky G 1965 *Solid State Commun.* **3** 299

[24] Binnenbruck H and Hausen A 1971 Optical properties of boron carbide and comparison with β-rhombohedral boron *Phys. Status Solidi* b **47** 153

[25] Schmechel R 1998 *Thesis* Gerhard Mercator University Duisburg, Germany

[26] Wood C 1985 Transport properties of boron carbide *AIP Conf. Proc.* **140** 206–15

[27] Wood C 1987 The transport properties of boron carbide prepared by different techniques *Proc. 9th Int. Symp. on Boron, Borides and Rel. Comp.* ed H Werheit (Duisburg: University Press) pp 213–22

[28] Aselage T L, Emin D and McCready S S 2001 Conductivities and Seebeck coefficients of boron carbides: softening bipolaron hopping *Phys. Rev.* B **64** 054302

[29] Aselage T L, Emin D and McCready S S 2000 Bipolaron hopping conduction in boron carbides *Phys. Status Solidi* b **218** 255

[30] Emin D 1986 Electronic transport in boron carbides *AIP Conf. Proc.* **140** 189
[31] Howard I A, Beckel C L and Emin D 1987 Bipolaron formation in B_{12} and $(B_{11}C)^+$ icosahedra *MRS Symp. Proc.* **97** 177
[32] Howard I A, Beckel C L and Emin D 1987 Bipolarons in boron icosahedra *Phys. Rev.* B **35** 2929
[33] Howard I A, Beckel C L and Emin D 1987 Bipolarons in boron-rich icosahedra: effect of carbon substitution *Phys. Rev.* B **35** 9265
[34] Emin D 1990 Electronic and vibrational hopping transport in boron carbides *AIP Conf. Proc.* **231** 65
[35] Emin D 1989 Theory of electronic and thermal transport in boron carbides *The Physics and Chemistry of Carbides, Nitrides and Borides* ed R Freer (Dordrecht: Kluwer–Academic) p 691
[36] Emin D 2006 Unusual properties of icosahedral boron-rich solids *J. Solid State Chem.* **179** 2791–8
[37] Werheit H 2006 Are there bipolarons in icosahedral boron-rich solids? *J. Phys.: Condens. Matter* submitted
[38] Werheit H, Janowitz C, Schmechel R, Tanaka T and Ishizawa Y 1997 Interband critical points of some icosahedral boron-rich solids *J. Solid State Chem.* **133** 132–9